Synthesis, characterization and DNA interaction studies of a new platinum(II) complex containing caffeine and histidine ligands using instrumental and computational methods

Nahid Shahabadi & Nazanin Moeini

View supplementary material ⍜

Accepted author version posted online: 28 May 2015.
Published online: 22 Jun 2015.

Submit your article to this journal ⍜

Article views: 59

View related articles ⍜

View Crossmark data ⍜

Taylor & Francis
Taylor & Francis Group

Synthesis, characterization and DNA interaction studies of a new platinum(II) complex containing caffeine and histidine ligands using instrumental and computational methods

NAHID SHAHABADI*†‡ and NAZANIN MOEINI†

†Department of Inorganic Chemistry, Faculty of Chemistry, Razi University, Kermanshah, Iran
‡Medical Biology Research Center (MBRC), Kermanshah University of Medical Sciences, Kermanshah, Iran

[Pt(Caffein)(Histidine)(Cl)]
+ ct-DNA
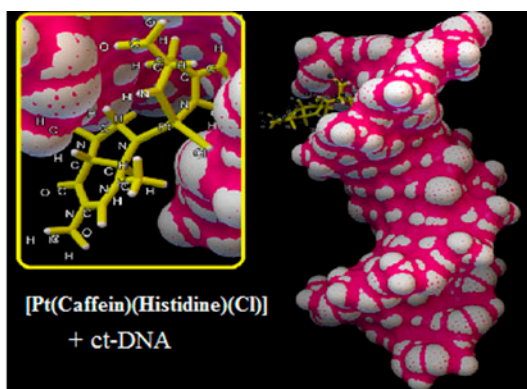
A new Pt(II) complex, [Pt(Caff)(His)(Cl)] (Caff is Caffeine (3,7-dihydro-1,3,7-trimethyl-1H-purine-2,6-dione) and His is L-Histidine), was synthesized and characterized using different physicochemical methods. The interaction of this complex with calf thymus DNA (ct-DNA) was investigated by absorption, emission, circular dichroism (CD), and viscosity measurements and molecular docking techniques. The calculated binding constant, K_b, was 5.3×10^3 M^{-1}. In fluorimetric studies, the enthalpy and entropy of the reaction between the complex and ct-DNA showed that the reaction is exothermic ($\Delta H = -184.07$ kJ mol^{-1}, $\Delta S = -551.97$ J mol^{-1} K^{-1}). CD spectra of DNA in the presence of different amounts of the complex showed little changes in both the negative and positive band intensities, which imply a non-intercalative mode between the DNA and the platinum complex. Furthermore, the study of molecular docking also indicated that the complex binds to DNA via a groove binding mode.

Keywords: Platinum complex; Caffeine; L-Histidine; ct-DNA; Groove binding mode

---

*Corresponding author. Email: n.shahabadi@razi.ac.ir

1. Introduction

DNA is a major target for drugs and some harmful chemicals to be attacked. The interaction of small molecules with DNA is at the interface of chemistry and biology. Binding mechanism of small molecules with DNA has been identified as a key topic to be studied [1, 2]. Small molecules can react with DNA via covalent or non-covalent interactions, with interest generally focusing on the latter. There are several sites in the DNA molecule where such binding can occur: (i) intercalating between stacked base pairs, (ii) non-covalent groove binding, or (iii) electrostatic interaction with the negatively charged nucleic acid sugar-phosphate structure [3, 4]. Many anticancer, antibiotic and antiviral pharmaceuticals exert their primary biological effects by reversibly interacting with DNA [5, 6]. Therefore, the study of the action mechanism, trend in DNA-binding affinities, and optical properties of small molecules with DNA has significance in better understanding of their clinical activities and rational design of more powerful and selective anticancer pharmaceuticals.

Types of platinum antitumor compounds are cis-platin, carboplatin, and oxaliplatin. Cisplatin, cis-diammine dichloro platinum(II), is an anticancer drug widely used to treat a variety of tumors, especially those of the testes, ovaries, head, and neck [7–12]. The major target of cis-platin is DNA. Cis-platin becomes active by forming DNA adducts. It is
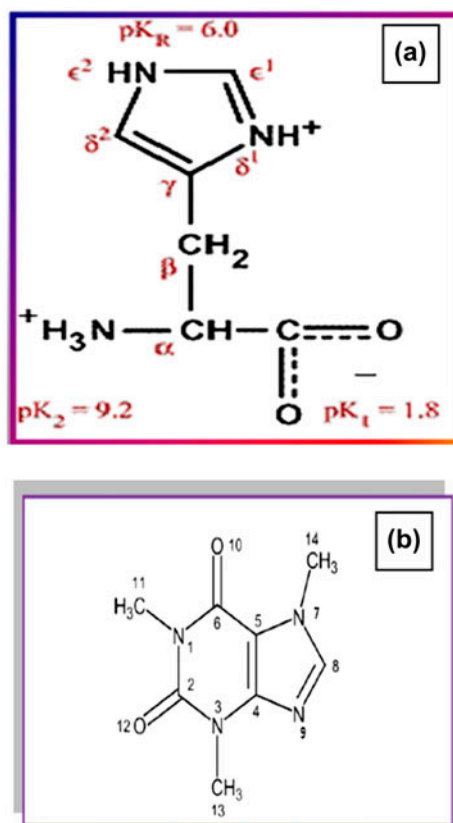

Figure 1.   (a) Molecular structure of histidine. (b) Molecular structure of caffeine.

probably via coordination to the N_7 position of a guanine base, but the details of the attachment and the mechanism of its effect on the cancer cell are unknown. Formation of cis-platin–DNA adducts interferes with cell cycle check points, cell replication, and transcription or regulation of signal transduction pathways. The outcome of these alterations is DNA damage and then cell death. It is interesting that trans isomer of platin is essentially inactive [13, 14]. Side effects, especially nephrotoxicity, of this drug limit its widespread use in high dose [15]. The need to develop new complexes with reduced nephrotoxicity and higher activity has stimulated the synthesis of many new complexes.

Histidine is an essential amino acid. It was initially thought that it was only essential for infants, but longer term studies established that it is also essential for adult humans [16]. L-Histidine behaves quite differently from the other amino acids in the interaction of the complexes with DNA. As an imidazole group of a histidine coordinates to a metal ion, it is expected that the histidine complex binds to DNA with a binding mode different from other amino acid complexes in which an amino nitrogen and a carboxyl oxygen are the coordinating groups [figure 1(a)] [17].

Caffeine is naturally found in plant sources, including coffee, cocoa, tea, cola nuts, guarana, etc. Caffeine (3,7-dihydro-1,3,7-trimethyl-1H-purine-2,6-dione) could be used to examine the coordination ability on the N_9 and $O=(C_6)$ sites as far as the N_7 one is blocked by the $-CH_3$ group [figure 1(b)]. It is a typical alkaloid belonging to the family of purine alkaloids. The formula is $C_8H_{10}N_4O_2$ and common name is trimethyl xanthine; it is soluble in water and organic solvents such as alcohol and chloroform. Pure form of caffeine is a white powder with a bitter taste but no odor [18]. Many studies have shown that caffeine may function in physical performance, energy expenditure, neuromuscular coordination, cognitive functioning, etc., leading to its clinical uses on obesity, fatigue, anxiety, attention deficit, Alzheimer's disease, etc. Nevertheless, higher doses of caffeine would produce adverse effects to healthy population, especially sensitive people, causing problems, such as anxiety, tremor, palpitations, insomnia, gastrointestinal disturbances, and increased blood pressure [19–21]. It is essential to understand the interactions between caffeine with metal transition ions in order to follow many biological processes. A few metal–caffeine complexes have shown significant antitumor activities on different animal cancer models and various types of malignant cell lines [22–24].

Therefore, to design improved drugs that target DNA and to investigate the effect of mixed-ligand complexes on the structure and conformation of DNA, we designed a Pt(II) complex, [Pt(Caff)(L-His)(Cl)] (in which Caff is caffeine (3,7-dihydro-1,3,7-trimethyl-1H-purine-2,6-dione and L-His is L-Histidine). Binding of this complex with calf thymus DNA (ct-DNA) was studied by electronic absorption spectroscopy, fluorescence spectroscopy, circular dichroic spectral, viscosity measurements, and computational method.

2. Experimental

2.1. *Materials*

Chemicals, K_2PtCl_4, hydrazine dihydro chloride, caffeine, and histidine were purchased from Merck. Tris–HCl and ct-DNA were purchased from Sigma Co. Experiments were carried out in Tris–HCl buffer at pH 7.2. A solution of calf thymus DNA gave a ratio of UV absorbance at 260 and 280 nm more than 1.8, indicating that DNA was sufficiently free

from protein. The stock solution of DNA was prepared by dissolving DNA in 10 mM of the Tris–HCl buffer at pH 7.2. The DNA concentration (monomer units) of the stock solution (1×10^{-2} M per nucleotide) was determined by UV spectrophotometer in properly diluted samples using the molar absorption coefficient 6600 M^{-1} cm^{-1} at 258 nm. The stock solutions were stored at 4 °C and used over no more than 4 days.

2.2. Synthesis and characterization of platinum complex

Potassium tetrachloroplatinate(I1) react with caffeine in DMF at room temperature and at ~55 °C, respectively, and give 1 : l complexes according to the general equation:

$$'K_2MCl_4 + Caff \rightarrow K[MCaffCl_3] + KC1$$
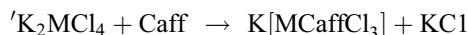
The monocaffeine complex of platinum, $K[PtCaffCl_3]$ is very unstable in water. This complex, however, is stabilized in the presence of the nucleosides adenosine (Ado), guanosine (Guo) and inosine (Ino) [25, 26]. An amount of 1 mmoL (0.155 g) of histidine was dissolved in 10 mL water and added to a solution of $[PtCl_3(Caff)]$ (1 mmoL) in small portions with vigorous stirring. The mixture was left at room temperature for several days. The precipitate was filtered and washed with water and air dried (yield: 77%). Based on the elemental analysis data, the structure was $[PtCl(Caff)(His)]$ complex. Anal. Found (%): C, 27.05; H, 4.1; N, 15.3. Calcd (%): C, 28.9; H, 3.72; N, 16.0.

2.3. Instrumentation

^1H and ^{13}C NMR spectra were recorded using a Bruker Avance DPX200 MHz (4.7T) spectrometer using D_2O as solvent. The elemental analysis was performed using a Heraeus CHN elemental analyzer.

UV–vis absorption measurements were carried out in pH 7.4 using a Tris–HCl buffer. The absorbance measurements were performed by keeping the DNA concentration constant (5×10^{-5} M) while varying the complex concentration (from 2.4 to 1.3×10^{-4} M). The spectra were recorded from 200 to 400 nm. Absorbance spectra were recorded using an HP spectrophotometer (Agilent 8453).

Fluorescence measurements were carried out with a JASCO spectrofluorimeter (FP 6200) by keeping the concentration of the complex constant (5×10^{-5} M) while varying the DNA concentration from 0 to 3×10^{-5} M (r_i = [DNA]/[complex] = (1.1, 1.4, 2, 2.2, 2.5, 2.8, 3.1) at three different temperatures (288, 298 and 310 K).

Circular dichroic spectra of DNA in the presence and absence of platinum(II) complex were obtained using a JASCO spectropolarimeter (J-810) at 25 °C using 0.5 cm (1 mL) path length quartz cuvette. CD measurements were recorded keeping the concentration of DNA constant (5×10^{-5} M) while varying the concentration of complex (r = [complex]/[DNA] = 0, 0.15, 0.96, 1.4).

In this study, a viscometer (SCHOT AVS 450), thermostated at 25 °C by a constant temperature bath, was used. Typically, 15.0 mL of buffer and 15.0 mL of DNA solution were transferred into the viscometer separately. Various concentrations of complex were added into the viscometer to give a specific mole ratio r (r = [complex]/[DNA]) while keeping the DNA concentration at 5.0×10^{-5} mol L^{-1} [27]. After thermal equilibration, the time of the solution's flowing through the capillary was determined $t_0 \pm 0.2$ s by a digital stopwatch. At

least three measurements were tested to calculate the average relative viscosity of the DNA solution. The data were presented as $(\eta/\eta_0)^{1/3}$ *versus* the mole ratio values, where η and η_0 are the viscosity of DNA in the presence and absence of the complex, respectively. Viscosity values were calculated from the observed flow time of DNA-containing solutions (t) and corrected for buffer solution (t_0), $\eta = (t - t_0)/t_0$.

2.4. *Molecular modeling*

MGL tools 1.5.4 with AutoGrid4 and AutoDock4 [28] were used to set up and perform blind docking calculations between the complex and DNA sequence d (CGCGAATTCGCG) 2 dodecamer (PDB ID: 1BNA) obtained from the Protein Data Bank. Receptor (DNA) and ligand (complex) files were prepared using AutoDock Tools. The DNA was enclosed in a box with a number of grid points in $x \times y \times z$ directions, $58 \times 74 \times 122$ and a grid spacing of 0.375 Å. The center of the grid set to 14.78, 20.976, and 8.807 Å. Lamarckian genetic algorithms, as implemented in AutoDock, were employed to perform docking calculations. The structures of molecules were drawn and optimized using Spartan '10 package. All the molecular images and animations were produced using PyMol [29].

3. Results and discussion

3.1. *Synthesis and characterization of platinum complex*

A new Pt(II) complex, [Pt(Caff)(His)(Cl)], was synthesized by modification of reported procedure [25]. The complex was characterized by theoretical and physicochemical methods. Calculations on the structure of the complex [$C_{14}H_{19}ClN_7O_4Pt$] (figure 2) were performed by Spartan '10 package method. The structure of the complex was obtained by PM6 method [30]. The point group of [$C_{14}H_{19}ClN_7O_4Pt$] was C_1. The results of the calculations demonstrated [$C_{14}H_{19}ClN_7O_4Pt$] has very distorted square planar arrangement around Pt (figure 2). The coordination bond angles were 91.20° [N_1-Pt_1-N_4], 7.99° [N_1-Pt_1-N_3], 113.76° [N_3-Pt_1-Cl_1], 110.71° [N_4-Pt_1-Cl_1], 110.55° [N_1-Pt_1-Cl_1], and 135.52°
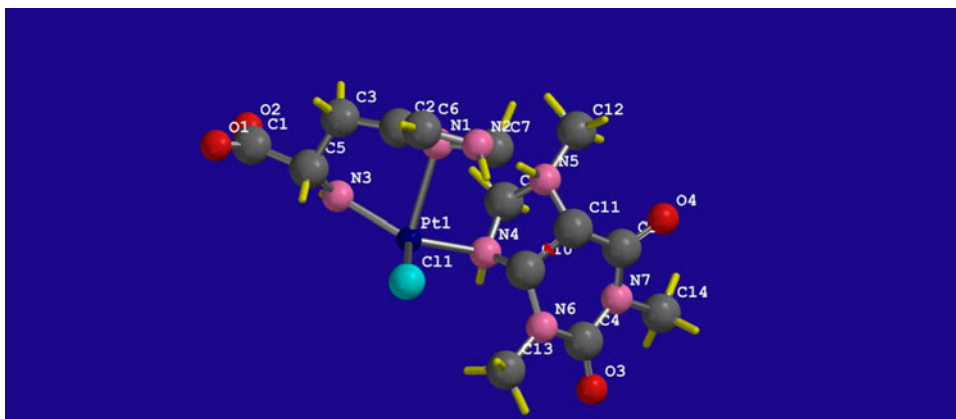

Figure 2.   Molecular structure of [Pt(Caff)(His)(Cl)].

[N_3-Pt_1-N_4]. Bond distances were 2.50 Å for Pt-N_1 distance, 2.06 Å for Pt-N_3, 2.10 Å for Pt-N_4 and 2.26 Å for Pt-Cl_1. The diagonal angles [N_3-Pt_1-N_4] and [N_3-Pt_1-Cl_1] were 135.52° and 113.76°, respectively, while in square planar structure, these angles are 180°. The strong distortion from the square planar geometry of complex was indicated.

The structure of the complex was also characterized by elemental analysis, UV–vis, IR and ^{1}H and ^{13}C NMR spectroscopic methods. The complex is air stable and readily soluble in water.

IR spectra of the ligands and Pt complex are shown in figure S1 (see online supplemental material at http://dx.doi.org/10.1080/00958972.2015.1055259). The bands of free caffeine at 1657 and 1699 cm^{-1} are assigned to υ(C=O) stretches. These bands shift about 3 cm^{-1} in the IR spectrum of Pt(II) complex. This result indicated that C=O groups are free from complexation. When coordination occurs through the carbonyl oxygen, the υ(C=O) frequency shifts to lower energy [31]. The 1599 and 1549 cm^{-1} bands in caffeine shifted to 1552 and 1497 cm^{-1} in the complex. The peak of νC = N (imidazole) in the ligand practically disappears in the complex. These data indicate a monodentate coordination of caffeine through N_9. Similar Zn^{2+} and Au complexes have been obtained and crystallographically refined [32]. The broad band of the N–H stretch in the spectrum of the complex (3108 cm^{-1}) was shifted to lower frequency as compared to L-Histidine (3126 cm^{-1}). This is indicative for coordination of the histidine to the Pt through the NH group. The υ(Pt-N) vibration is usually weak and difficult to assign. We have found a weak band at 537 cm^{-1} for υ(Pt-N) as reported for Pt(glycine)$_2$ in 549 cm^{-1} (table 1) [33].

The ^{1}H NMR spectra of caffeine, histidine, and Pt complex are shown in figure S2 and the data are provided in table 2. ^{1}H NMR spectra have shown proton signals at aliphatic (0– 4 ppm) and aromatic (7–10 ppm) regions. The peak at δ = 4.8 ppm is related to D_2O solvent. The signal of H (D) in caffeine was detected at 7.9 ppm, whereas in the complex spectrum, it is at 8.1 ppm, indicative for coordination of the caffeine to Pt through N. The signals of H (G, H) in histidine were detected at 4.06 and 7.4 ppm, whereas in the complex, at 4.6 and 7.9 ppm, respectively, which indicated coordination through N and NH_2 in histidine. There is no appreciable change in other signals of the complex. The ^{13}C NMR spectrum of the complex was also recorded [figure S2(d)] and compared with that of free caffeine and histidine [26]. It is evident from these spectra that the ligands attached to platinum (table 1).

Electronic spectra of the ligands and complex (10^{-5} M) were recorded in Tris–HCl buffer at room temperature. The electronic absorption spectrum of histidine exhibits an intense absorption at 204 nm, which is assigned to $n \rightarrow \pi^*$ transition of the drug. In the electronic absorption spectrum of Pt(II) complex, this band shifts to 209 nm. Caffeine exhibits an intense absorption at 206 nm, which is assigned to $n \rightarrow \pi^*$ transition of drug, while in the electronic absorption spectrum of platinum complex, this band shifted to 209 nm and decreasing absorbance intensity. Also, an intense absorption of caffeine at 273 nm disappeared in the platinum complex (figure S3). Therefore, the absorption spectrum confirms the suggested structure for the platinum complex.

Table 1.   IR data for free ligands and Pt complex (in cm^{-1}).

Compound	υ(C=O)	υ(C–N)	υ(Pt-N)	υ(N–H)
Caffeine	1657; 1699	1559; 1549	–	3448
L-Histidine	1590; 1634	1569	–	3126
Pt complex	1654; 1702	1552; 1479	537	3180; 3108

Table 2.   Selected ^{1}H and ^{13}C NMR spectral data (in ppm).

Compound	H_A	H_B	H_C	H_D	C2	C4	C5	C6	C8	Me
Caffeine	3.89	3.4	3.3	7.9	152.9	148.7	108.1	156.4	144.2	28–34
Pt complex	3.86	3.4	3.36	8.1	152.8	150.1	112	–	–	~34

Compound	H_E	H_F	H_G	H_H	Cα	Cβ	Cγ		Cε	C=O
L-Histidine	3.3	8.6	4.06	7.4	53.75	28.78	134.67		117.88	170
Pt complex	3.27	–	4.6	7.9	50.3	24.6	128.9		114.6	171

3.2. *DNA interaction studies of platinum complex*

3.2.1. UV–vis spectroscopy. Electronic absorption spectra are employed to study the binding of complexes to DNA. Complex absorption titration experiments were carried out by keeping the concentration of DNA constant (5×10^{-5}) while varying the complex concentration from 2.4×10^{-5} to 1.3×10^{-4} M (r_i = [complex]/[DNA] = 0.48, 0.94, 1.8, 2.6). Absorbance values were recorded after each successive addition of DNA solution and equilibration (*ca.* 2 min) (figure 3). The value of the binding constant (K) was obtained from the DNA absorption at 260 nm according to equation (1) for weak binding affinities,

$$\frac{1}{A - A_0} = \frac{1}{A_\infty - A_0} + \frac{1}{K(A_\infty - A_0)} \times \frac{1}{[\text{COM}]} \tag{1}$$

where A_0 is the absorbance of DNA at 260 nm in the absence of the platinum complex, A_∞ is the final absorbance of complex-DNA adduct, and A is the recorded absorbance at different platinum complex concentrations. The linearity of the double reciprocal plot of $1/(A - A_0)$ *versus* 1/[complex] (figure S4) and the binding constant (K) can be estimated from the ratio of intercept to the slope [34]. The binding constant for complex-DNA adduct was calculated as 5.4×10^3 at 25 °C. The K_b value for the complex is comparable to those
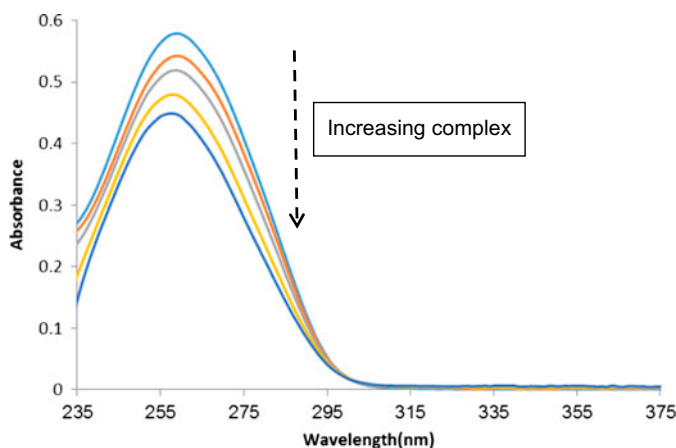

Figure 3.   UV/vis spectrum of ct-DNA (5×10^{-5} mol L^{-1}) in the presence of different concentrations of complex (r_i = [complex]/[DNA] = 0.48, 0.94, 1.8, 2.6).

observed for complexes like, $[Co(phen)_3]^{3+}$ $(1.6 \times 10^4 \text{ M}^{-1})$ [35]; $[Ru(phen)_3)]^{2+}$ $(0.55 \times 10^4 \text{ M}^{-1})$ [36]; $[Ni(DIP)_3]^{2+}$ (4.34×10^4) [37].

The UV–vis spectrum shown in figure 3 demonstrates that the platinum complex causes a hypochromic effect on the DNA spectrum at different concentrations. Hypochromism results from the contraction of DNA in the helix axis, as well as from the change in the DNA conformation, while hyperchromism results from the damage of the DNA double-helix structure. This hypochromism effect is consistent with binding of platinum complex to the grooves of DNA via hydrogen bonds as well as binding to backbone phosphate oxygen via electrostatic interaction. Thus, the overall conformation changes of DNA structure may be a combination of a groove mode of binding through hydrogen bonds and electrostatic interaction [38–40]. Since DNA possesses several hydrogen bonding sites in the minor as well as major grooves, and the platinum(II) complex contains a NH group, there could be hydrogen bonding between platinum(II) complex and the base pairs in DNA [41]. In addition, the platinum(II) complex, which possesses methylene groups, can bind to DNA by van der Waals interaction between the methylene groups and the thymine methyl group [42]. No red shift or isosbestic points are observed in the UV spectrum, which represents that the binding mode is not intercalative binding [43].

3.2.2. Fluorescence studies. Platinum complex has an emission maximum at 382 nm on excitation at 340 nm (absorption maximum). The fluorescence titration spectra of the platinum complex in the absence and presence of DNA at 25 °C are given in figure 4. [Pt(Caff) (His)(Cl)] is luminescent in the absence of DNA and does show appreciable increase in emission upon addition of DNA. The enhancements of emission intensity imply that the compound can interact with DNA base pairs. As a result, the complex is protected from solvent water by the hydrophobic environment inside the DNA helix; the accessibility of solvent water molecules to the complex is reduced.

The enhancement constant can be obtained by equation (2) [44]:

$$F_0/F = 1 - K_E[E] \qquad (2)$$

If a dynamic process is part of the enhancing mechanism, the above equation can be written as follows [44]:
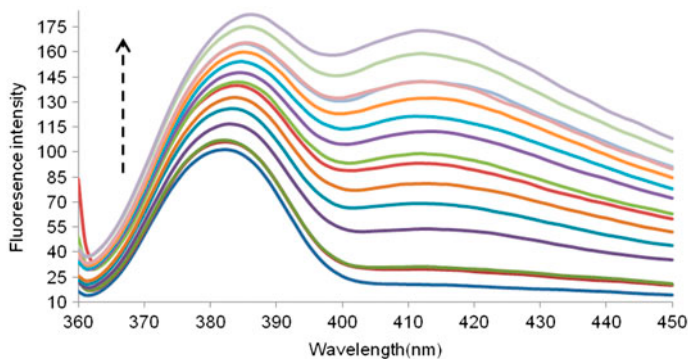

Figure 4.   Fluorescence spectra of the complex $(1.0 \times 10^{-5}$ M) in the absence and presence of increasing amounts of ct-DNA.

$$F_0/F = 1 - K_D[E] = 1 - K_B\tau_0[E] \tag{3}$$

where K_D is the dynamic enhancement constant, K_B is the bimolecular enhancement constant, τ_0 is the lifetime of the fluorophore in the absence of the enhancer, and $[E] = [DNA]$, the concentration of enhancer. Since fluorescence lifetimes are typically near 10^{-8} s, the bimolecular enhancement constant (K_B) was calculated from $K_D = K_B\tau_0$ [44]. The dynamic enhancement constant of the Pt(II) complex at different temperatures were calculated using equation (3); the results are shown in table 3. Plot of F_0/F *versus* [DNA] at different temperatures is shown in figure S5. K_D and K_B increase as temperature increases, indicating that the mechanism of the quenching may be a dynamic quenching. However, K_B is much larger than 2.0×10^{10} L mol^{-1} s^{-1}, suggesting that the quenching process may be static quenching. Two kinds of quenching mechanism demonstrate some differences that can be distinguished experimentally, such as change in the UV–visible spectrum of DNA and temperature dependence of the quenching constant [44]. According to the theory mentioned, a complex of DNA and the platinum complex forms in static quenching, so there will be some changes in the UV–visible spectrum of DNA.

The binding constant (K_f) and the binding stoichiometry (n) for the complex formation between Pt complex and DNA were measured using equation (4).

$$\log (F - F_0)/F = \log K_f + n \log[DNA] \tag{4}$$

Here F_0 and F are the fluorescence intensities of the fluorophore in the absence and presence of different concentrations of DNA, respectively. The linear equations of $\log (F - F_0)/F$ *versus* log [DNA] at different temperatures are shown in table 3. The values of K_f clearly underscore the remarkably high affinity of platinum complex to DNA. The value of K_f for complex at room temperature is comparable to arctiin (2.5×10^3 M^{-1}) mesalamine (0.237×10^3 M^{-1}), which binds to DNA in a groove mode [45, 46].

The plot of ln K_f *versus* $1/T$ allows the enthalpy (ΔH), entropy (ΔS) (equation 5), and free energy (ΔG) change by the van't Hoff equation (equation 6) to be determined, assuming that the enthalpy change (ΔH) is free of temperature over the range of applied temperatures.

$$\ln K = -\frac{\Delta H}{RT} + \frac{\Delta S}{R} \tag{5}$$

$$\Delta G = \Delta H - T\Delta S \tag{6}$$

Table 3 exhibits the thermodynamic values of Pt complex. According to the data of enthalpy changes (ΔH) and entropy changes (ΔS), the model of interaction between the drug and DNA can be concluded [47]: (1) $\Delta H > 0$ and $\Delta S > 0$, hydrophobic forces; (2)

Table 3. The quenching constants, binding constants (K_f), the number of binding sites (n), and thermodynamic parameters for the binding of platinum complex to ct-DNA.

T (K)	K_D (L mol^{-1}) $\times 10^4$	K_B (L mol^{-1}) $\times 10^{12}$	n	K_f	ΔG^0 (kJ mol^{-1})	ΔH^0 (kJ mol^{-1})	ΔS^0 (J mol^{-1} K^{-1})
288	507	507	1.35	1.9×10^5	−27,865	−184.072	−551.96
298	693	693	0.78	1.1×10^3	−19,586	−184.072	−551.96
310	744	744	0.66	3×10^2	−12,962	−184.072	−551.96

$\Delta H < 0$ and $\Delta S < 0$, van der Waals interaction and hydrogen bonds; (3) $\Delta H < 0$ and $\Delta S > 0$, electrostatic interactions [48]. The negative value of ΔG revealed the DNA interaction is spontaneous; the negative ΔH and ΔS values indicated that van der Waals interaction and hydrogen bonds play main roles in the binding of platinum complex to DNA.

3.2.3. Competitive binding between methylene blue (MB) and platinum complex for the interaction with DNA. To support the spectral results, a competitive study using MB was done. MB is a well-known intercalator, which is often used as a spectral probe to establish the mode of binding of small molecules to double-helical DNA. The fluorescence of MB decreases after binding with DNA due to intercalation [49]. Like MB, if Pt(II) complex intercalates into the helix of DNA, it would compete with MB for the intercalation sites in DNA, and lead to a significant increase in the fluorescence intensity of the MB–DNA complex but there is no significant displacement of MB by Pt(II) complex reflecting the absence of intercalative binding. As there is evidence of complex formation from other experiments, a groove-binding mode could be ascribed to it. This has also been substantiated by other experimental studies as well as DNA-complex docking (figure 5).

3.2.4. CD spectral studies. Circular dichroism (CD) is a sensitive technique to monitor the conformational changes in proteins and DNA. The observed CD spectrum of natural DNA consists of a positive band at 275 nm due to base stacking and a negative band at 245 nm due to helicity, which is characteristic of DNA in right-handed B form [50]. The effect of [Pt(Caff)(L-His)(Cl)] on the conformation of secondary structure of DNA was studied by keeping the concentration of DNA constant at 5×10^{-5} M, while varying the concentration of the complex in a buffer solution of 50 mM of Tris ($r_i = 0.0$, 0.15, 0.96, 1.4). As shown in figure 6, in the presence of the complex, both the negative and positive band intensities of the CD spectra of DNA show little change, implying a non-intercalative mode between DNA and platinum complex. These changes show stabilization of the right-handed B form of DNA [51].
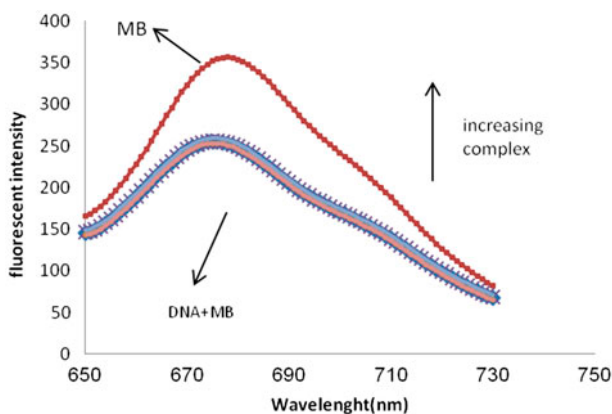

Figure 5. Fluorescence spectra of the competition between Pt(II) complex and MB; [MB] = 10^{-5}, [DNA] = 1.6×10^{-3} and [Complex] = 1×10^{-3}–4.5×10^{-3} M.
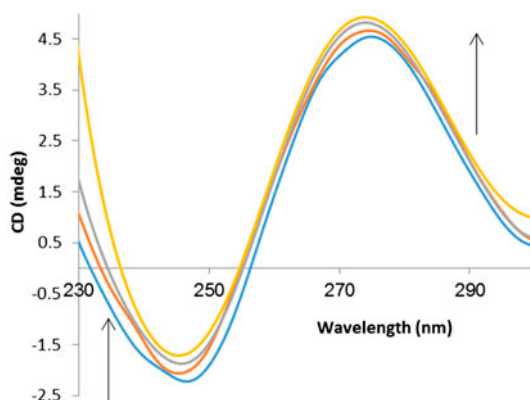
Figure 6. CD spectra of DNA (5×10^{-5} M) in Tris–HCl buffer in the presence of increasing amounts of the complex (r_i = [complex]/[DNA] = 0.0, 0.15, 0.96, 1.4).

3.2.5. Viscosity measurements. Viscosity is an effective tool to decide the binding mode of drug and ct-DNA. A classical intercalation binding demands the space of adjacent base pairs to be large enough to accommodate the bound ligand and elongates the double helix, resulting in an increase of ct-DNA viscosity [52]. However, a partial non-classical intercalation of ligands can bend (or kink) the ct-DNA helix and reduce its effective length and its viscosity [53]. There is little effect on the viscosity of ct-DNA if the electrostatic or groove surface binding occurs in the binding process [54]. The ct-DNA viscosity experiments were performed at 25 °C. Increasing amounts of the complex (r_i = 0–1.4) were used to evaluate viscosity η of the ct-DNA. The values of relative specific viscosity $(\eta/\eta_0)^{1/3}$ *versus* r_i (r_i = [complex]/[DNA]) were plotted (figure 7). Little change on the viscosity of ct-DNA showed that the complex bound to DNA by groove binding such as paeoniflorin [55].

3.2.6. Molecular docking studies on the interaction mechanism of complex with DNA. Computer docking techniques play an important role in drug design and elucidation of mechanism. The flexible docking programs, AutoDock and molecular operating environ-
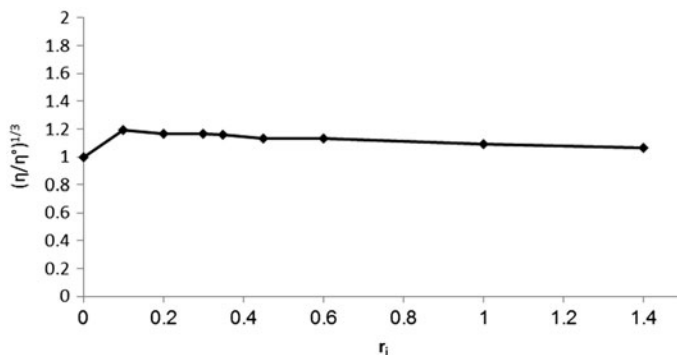

Figure 7. Effect of increasing amounts of Pt complex on the viscosity of ct-DNA (5×10^{-5} M) in Tris–HCl buffer (pH 7.4) (r_i = 0.0, 0.1, 0.2, 0.3, 0.35, 0.45, 0.6, 1, 1.4).

ment help in predicting favorable protein–ligand complex structures with a reasonable accuracy and speed. These docking programs, when used prior to experimental screening, can be considered as powerful computational filters to reduce labor and cost needed for development of effective medicinal compounds. When used after experimental screening, they can help in better understanding of bioactivity mechanisms [56]. The docking is important in the study of various properties associated with protein–ligand interactions, such as binding energy, geometry complementarily, electron distribution, hydrogen bond donor, acceptor properties, hydrophobicity, and polarizability [57]. From the docking results with the optimal energy, it was found that the complexes inserted into the minor groove of DNA fragments and hydrogen bonds play the main role in the binding of complex to DNA. There is a hydrogen bond between oxygen of the complex with $O_{4'}$-DG-12 and bond length of 2.83 Å (figure 8). As shown in figure 9 from the docking calculation, the conformer with minimum binding energy is picked up from the nine minimum energy conformers from the 200 runs [58]. The data for the conformers are listed in table 4. The initial conformation was taken from one of the lowest binding energy docking conformations (table 4) (figure 9). From the results of nine sets, almost all the binding sites of complex were located in the groove of double-helix DNAs. The binding constant obtained by UV–visible method was correlated with the free binding energy of docked model. Basic formula of binding constant and Gibbs free energy is:

$$\Delta G = -\text{RT} \ln K \tag{7}$$

The binding constant obtained by UV–visible (5.3×10^3 M^{-1}) matches roughly to the binding constant calculated by docked complex-DNA model (10.6×10^3 M^{-1}). Hence, it can be concluded that complex-DNA docked model is in approximate correlation with our experimental results [59].
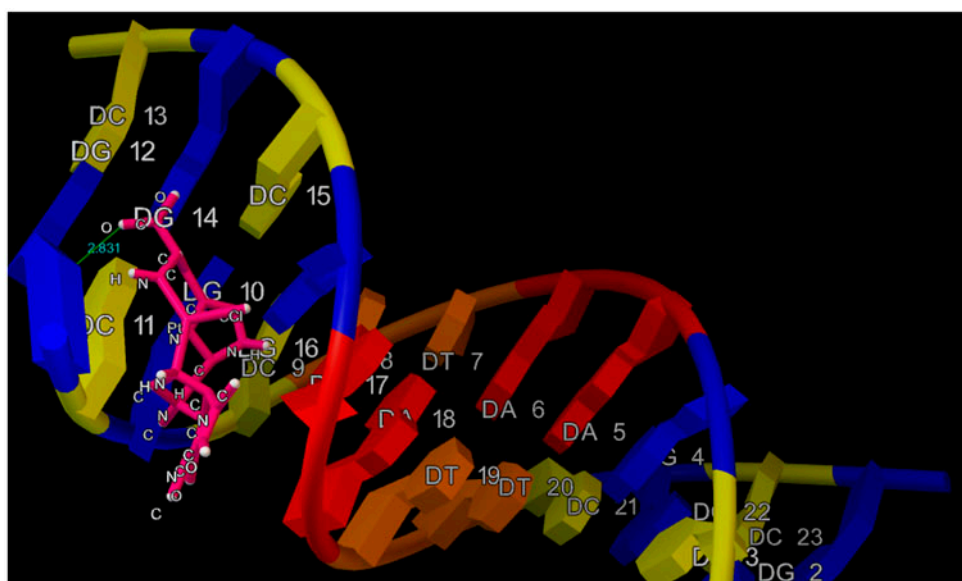

Figure 8.   Molecular modeling of the hydrogen-bonding interactions between metal complex and ct-DNA.
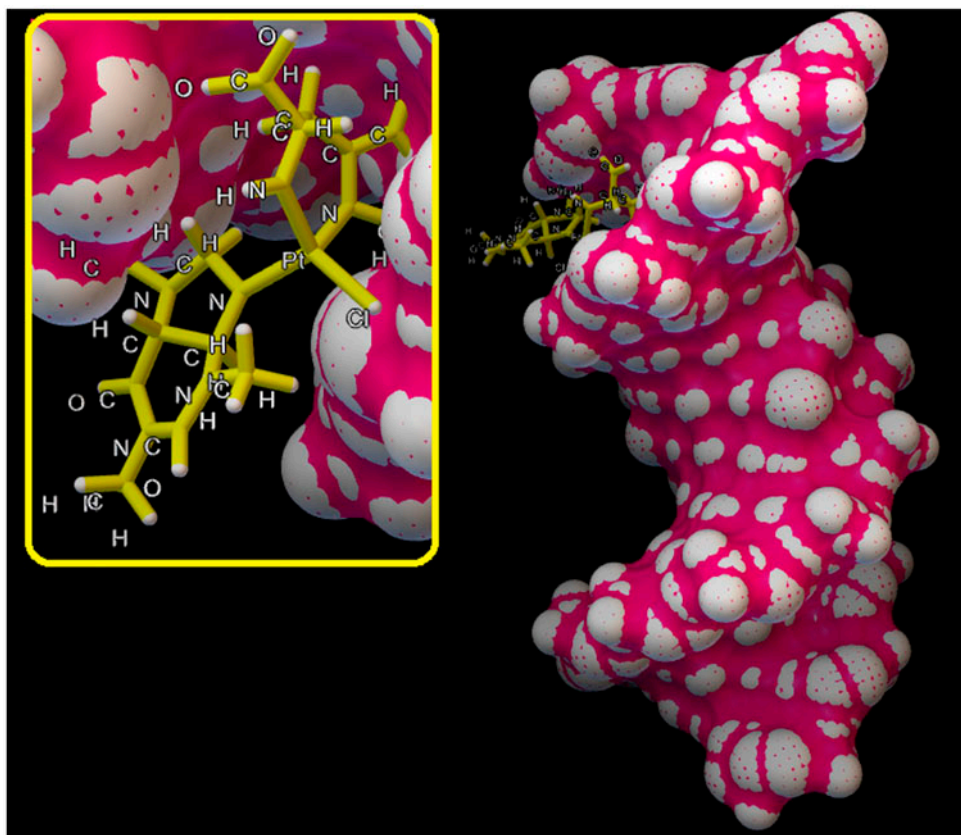
Figure 9.   Molecular docking perspective of complex with the minor groove of DNA.

Table 4.   Docking summary of DNA with complex by the AutoDock program generating different ligand conformers using a Lamarkian GA.

Rank	Run	Binding energy (kcal M^{-1})	^aK_i (μM)	K_a (M^{-1})	Cluster rmsd	Reference rmsd
1	33	−6.08	34.91	29.86×10^3	0.00	31.17
2	28	−6.03	39.96	27.43×10^3	0.00	26.07
3	74	−6.03	38.09	27.43×10^3	0.00	26.07
4	76	−6.03	37.99	27.43×10^3	0.00	26.07
5	173	−5.87	49.79	20.92×10^3	0.00	30.96
6	121	−5.77	59.11	17.65×10^3	0.00	29.85
7	133	−5.59	80.01	13.01×10^3	0.00	27.97
8	197	−5.55	86.14	12.16×10^3	0.00	32.02
9	**12**	**−5.47**	**97.89**	**10.6×10^3**	**0.00**	**29.12**

^aK_i is the inhibition constant.

4. Conclusion

A new Pt(II) complex, [Pt(Caff)(His)(Cl)], has been synthesized and characterized by elemental analysis, UV–vis, IR, ^{1}H, and ^{13}C NMR spectroscopy and computational method. The results suggest that the platinum complex binds to ct-DNA via groove binding mode. The interaction occurrence is supported by the following findings:

(1) The binding constant obtained by UV–vis (5.3×10^3 M^{-1}) matches roughly to the binding constant calculated by docked platinum complex-DNA model (10.6×10^3 M^{-1}). Hence, it can be concluded that platinum complex-DNA docked model is in approximate correlation with our experimental results.

(2) In absorption spectrum of [Pt(Caff)(His)(Cl)], as the concentration of DNA increased, hypochromism of the absorption band is observed.

(3) The platinum complex had little effect on the viscosity of ct-DNA.

(4) Increase in the fluorescence intensity of the ct-DNA upon adding the complex. The thermodynamic parameters ($\Delta H = -184.072$ kJ mol^{-1}, $\Delta S = -551.966$ J mol^{-1} K^{-1}) indicated that hydrogen bond and van der Waals play main roles in the binding of Pt complex to ct-DNA.

(5) No significant displacement of MB bound to DNA with the Pt complex indicates the absence of intercalation.

(6) In the presence of the complex, both the negative and positive band intensities of the CD spectrum of DNA show little change, implying a non-intercalative mode between DNA and platinum complex.

(7) Complex-DNA docked model is in approximate correlation with our experimental results.

Acknowledgment

Disclosure statement

No potential conflict of interest was reported by the authors.

References

[1] A. Hartwig. *Chem. Biol. Interact.*, **184**, 269 (2010).
[2] P.G. Mantle, V. Faucet-Marquis, R.A. Manderville, B. Squillaci, A. Pfohl-Leszkowicz. *Chem. Res. Toxicol.*, **23**, 89 (2010).
[3] A.M. Pyle, J.P. Rehmann, R. Meshoyrer, C.V. Kumar, N.J. Turro, J.K. Barton. *J. Am. Chem. Soc.*, **111**, 3051 (1989).
[4] E.C. Long, J.K. Barton. *Acc. Chem. Res.*, **23**, 271 (1990).
[5] I. Haq. *Arch. Biochem. Biophys.*, **403**, 1 (2002).
[6] J. Chen, X.Q. Lu. *Talanta*, **79**, 129 (2009).
[7] H. Ali, J.E. van Lier. *Chem. Rev.*, **99**, 2379 (1999).
[8] S. Roy, J.A. Westmaas, K.D. Hagen, G.P. van Wezel, J. Reedijk. *J. Inorg. Biochem.*, **103**, 1288 (2009).

 [9] A.Y. Louie, T.J. Meade. *Chem. Rev.*, **99**, 2711 (1999).
[10] H. Sakurai, Y. Kojima, Y. Yoshikawa, K. Kawabe, H. Yasu. *Coord. Chem. Rev.*, **226**, 187 (2002).
[11] W. Volkert, T. Hoffman. *Chem. Rev.*, **99**, 2269 (1999).
[12] P.M. Takahara, C.A. Frederick, S.J. Lippard. *J. Am. Chem. Soc.*, **118**, 12309 (1996).
[13] A. Basu, S. Krishnamurthy. *J. Nucleic Acids*, **16**, 201367 (2010).
[14] A.L. Pinto, S.J. Lippard. *Biochim. Biophys. Acta*, **780**, 167 (1985).
[15] R.F. Ozols, R.C. Young. *Semin. Oncol.*, **12**, 21 (1985).
[16] J.D. Kopple, M.E. Swendseid. *J. Clin. Invest.*, **55**, 881 (1975).
[17] R. Nagane, M. Chikira, M. Oumi, H. Shindo, W.E. Antholine. *J. Inorg. Biochem.*, **78**, 243 (2000).
[18] I. Bojidarka. *Turk. J. Chem.*, **31**, 97 (2007).
[19] M. Hadjicharalambous, E. Georgiades, L.P. Kilduff, A.P. Turner, F. Tsofliou, Y.P. Pitsiladis. *J. Sports Sci.*, **24**, 875 (2006).
[20] S.R. McClaran, T.J. Wetter. *J. Int. Soc. Sports Nutr.*, **4**, 11 (2007).
[21] P. Hewlett. *Human Psychopharmacol.: Clin. Exp.*, **22**, 339 (2007).
[22] I.H. Hall, R.W. Durham, M.J. Tram, S. Mueller, B.M. Ramachandran, L.G. Sneddon. *J. Inorg. Biochem.*, **93**, 125 (2003).
[23] M.N. Rilavarasi, S. Rao, M.R. Udupa. *Chem. Sci.*, **109**, 79 (1997).
[24] J. Piatkowski, H. Podsiadly, K. Bukietynska. *J. Biochem.*, **141**, 545 (2007).
[25] G. Pneumatikakis. *Inorg. Chim. Acta*, **93**, 5 (1984).
[26] P. Tsiveriotis, N. Hadjiliadis, G. Stavropoulos. *Inorg. Chim. Acta*, **261**, 83 (1997).
[27] R. Vijayalakshmi, M. Kanthimathi, V. Subramanian. *Biochim. Biophys. Acta*, **1475**, 157 (2000).
[28] G.M. Morris, R. Huey, W. Lindstrom, M.F. Sanner, R.K. Belew, D.S. Goodsell, A.J. Olson. *J. Comput. Chem.*, **30**, 2785 (2009).
[29] W.L. DeLano, *The PyMOL Molecular Graphics System*, DeLano Scientific, San Carlos, CA. http://py mol.sourceforge.net (2004).
[30] *Spartan '10-Quantum Mechanics Program: (PC/x86) 1.1.0v4*, Wavefunction, USA (2011).
[31] N. Raman, K. Pothiraj, T. Baskaran. *Mol. Struct.*, **1000**, 135 (2011).
[32] Z.-M. Jin, L. Li, M. Hu, H. Su, C. Tong. *Acta Cryst.*, **61**, 1849 (2005).
[33] N. Sarı, E. Antepli, D. Nartop, N.K. Yetim. *J. Mol. Sci.–IJMS*, **13**, 11870 (2012).
[34] S. Sharma, S. Singh, M. Chandra, D.S. Pandey. *J. Inorg. Biochem.*, **99**, 458 (2005).
[35] E.C. Long, J.K. Barton. *Acc. Chem. Res.*, **23**, 271 (1990).
[36] N. Zhao, X.M. Wang, H.Z. Pan, Y.M. Hu, L.S. Ding. *Spectrochim. Acta Part A: Mol. Biomol. Spectro.*, **75**, 1435 (2010).
[37] N. Shahabadi, S. Mohammadi, R. Alizadeh. *Bioorg. Chem. Appl.*, **2011**, 1–8 (2011).
[38] J. Liu, T. Zhang, T. Lu, L. Qu, H. Zhou, Q.L. Zhang. *J. Inorg. Biochem.*, **91**, 269 (2002).
[39] C.L. Liu, J.Y. Zhou, Q.X. Li, L.J. Wang, Z.R. Liao, H.B. Xu. *J. Inorg. Biochem.*, **75**, 233 (1999).
[40] M.T. Carter, M. Rodriguez, A.J. Bard. *J. Am. Chem. Soc.*, **111**, 8901 (1989).
[41] T.R. Li, Z.Y. Yang, B.D. Wang, D.D. Qin. *Eur. J. Med. Chem.*, **43**, 1688 (2008).
[42] P.U. Maheswari, V. Rajendiran, M. Palaniandavar, R. Thomas, G.U. Kulkarni. *Inorg. Chim. Acta*, **359**, 4601 (2006).
[43] J. Sun, S. Wu, Y. An, J. Liu, F. Gao, L.N. Ji, Z.W. Mao. *Polyhedron*, **27**, 2845 (2008).
[44] B.K. Sahoo, K.S. Ghosh, S. Dasgupta. *Biopolymers*, **91**, 108 (2008).
[45] Y. Sun, H. Zhang, S. Bi, X. Zhou, L. Wang, Y. Yan. *J. Lumin.*, **131**, 2299 (2011).
[46] N. Shahabadi, S. Moradi, F. Kheirdoosh. *Photochem. Photobiol. B. Biol.*, **128**, 20 (2013).
[47] V.A. Izumrudov, M.V. Zhiryakova, A.A. Goulko. *Langmuir*, **18**, 10348 (2002).
[48] S. Bi, C. Qiao, D. Song, Y. Tian, D. Gao, Y. Sun, H. Zhang. *Sens. Actuators B: Chem.*, **119**, 199 (2006).
[49] S. Nafisi, A.A. Saboury, N. Keramat, J.F. Neault, H.A. Tajmir-Riahi. *J. Mol. Struct.*, **827**, 35 (2007).
[50] V.I. Ivanov, L.E. Minchenkova, A.K. Schyolkina, A.I. Poletayev. *Biopolymers*, **12**, 89 (1973).
[51] F.H. Li, G.H. Zhao, H.X. Wu, H. Lin, X.X. Wu, S.R. Zhu, H.K. Lin. *J. Inorg. Biochem.*, **100**, 36 (2006).
[52] L.S. Lerman. *J. Mol. Biol.*, **3**, 18 (1961).
[53] L. Kapicak, E.J. Gabbay. *J. Am. Chem. Soc.*, **97**, 403 (1975).
[54] H. Deng, H. Li, H. Xu, L.N. Ji. *Acta Chim. Sinica*, **60**, 2159 (2002).
[55] G. Zhang, P. Fu, J. Pan. *J. Lumin.*, **134**, 303 (2013).
[56] F. Perveen, R. Qureshi, A. Shah, S. Ahmed, F. Latif Ansari, S. Kalsoom. Pharmaceuticals, 1, 1 (2011).
[57] A.A. Reda, A.N. Ammar, M.A. Alaghaz. *J. Electrochem. Sci.*, **8**, 8686 (2013).
[58] B. Sudhamalla, M. Gokara, N. Ahalawat, D.G. Amooru, R.J. Subramanyam. *J. Phys. Chem. B*, **114**, 9054 (2010).
[59] A. Abderrezak, P. Bourassa, J.S. Mandeville, R. Sedaghat-Herati, H.A. Tajmir-Riahi. *PLoS ONE*, **7**, e33102 (2012).